Available online at www.sciencedirect.com
SCIENCE DIRECT
Journal of Catalysis 230 (2005) 166–172
JOURNAL OF CATALYSIS
www.elsevier.com/locate/jcat

Low-pressure methanol oxidation over a Cu(110) surface under stationary conditions: (I) reaction kinetics

L. Zhou, S. Günther, R. Imbihl *

Institut für Physikalische Chemie und Elektrochemie, Universität Hannover, Callinstrasse 3-3a, D-30167 Hannover, Germany

Received 13 October 2004; revised 25 November 2004; accepted 29 November 2004

Abstract

The steady-state kinetics of methanol oxidation over Cu(110) have been studied in the 10^{-7} to 10^{-3} mbar range. H_2, H_2O, and CO_2 are found in addition to the main product formaldehyde. The reactive sticking coefficient of methanol reaches 0.2. A pronounced hysteresis is observed when the temperature is cycled. Our data indicate the presence of two rate maxima, one at ≈400–520 K and the other at ≈900 K. The amplitude of the low-temperature reactivity peak decreases with increasing total pressure, vanishing beyond 10^{-3} mbar. High oxygen partial pressures led to a poisoning of the reaction, which was apparently caused by the inhibitory effect of high oxygen coverage on methanol adsorption.

Keywords: Copper(110); Methanol oxidation; Formaldehyde; Stationary kinetics; Hysteresis; Pressure gap

1. Introduction

The interaction of methanol with copper surfaces is a key mechanistic step in several technologically important catalytic processes, such as methanol synthesis from "syngas" over Cu/ZnO catalysts and methanol steam reforming over Al_2O_3-supported Cu/ZnO [1–4]. High yields with partial oxidation of methanol to formaldehyde have been obtained with copper catalysts, although in industry silver is still mainly used for that purpose.

A significant number of both high-pressure studies and low-pressure single-crystal investigations have been published that focused on various aspects of methanol oxidation over copper surfaces. The main topics were (i) formulation of a reaction mechanism based on the presence of methoxy and formate intermediates [5–11], (ii) the identification of the active surface phases and surface species with the use of in situ techniques [12–15], and (iii) establishing the role of strain in determining the catalytic activity of copper under the conditions of real catalysis [3].

For product formation the following reactions can be formulated, in which formaldehyde is produced via dehydrogenation (1) or oxidative dehydrogenation (2); alternatively, total combustion to CO_2 may occur (3) [16,17]

$$CH_3OH \rightarrow CH_2O + H_2, \quad (1)$$

$$CH_3OH + \tfrac{1}{2}O_2 \rightarrow CH_2O + H_2O, \quad (2)$$

$$CH_3OH + \tfrac{3}{2}O_2 \rightarrow CO_2 + 2H_2O. \quad (3)$$

But reaction (1) is purely formal because this reaction does not take place on a clean copper surface and requires oxygen to proceed [15].

Single-crystal studies with Cu(110) as a catalyst have been conducted with temperature-programmed desorption (TPD), molecular beam techniques, and scanning tunneling microscopy (STM) [5–11]. These techniques were typically applied under nonstationary conditions with sequential dosing and in temperature-programmed experiments. From the observation of ordered adlayers of reactive intermediates with STM, a number of detailed insights into the reaction mechanism could be obtained, but it remained unclear how

* Corresponding author. Fax: +49 511 762 4009.
E-mail address: imbihl@pci.uni-hannover.de (R. Imbihl).

0021-9517/$ – see front matter © 2004 Published by Elsevier Inc.
doi:10.1016/j.jcat.2004.11.039

much these structures really determine the reactivity of the Cu(110) surface [7–11]. One way to attack this problem is to measure the reaction kinetics under stationary conditions, because any detailed mechanism must of course be consistent with the macroscopic kinetics.

For this reason we study the steady-state kinetics of the reaction in the low-pressure range from 10^{-7} to 10^{-3} mbar. Under these conditions the reaction is practically isothermal and surface reaction steps rather than mass transport through the gas phase limit the reaction. A second, more general goal is to establish a bridge between the low-pressure single-crystal studies and the high-pressure kinetics. Therefore we systematically varied the total pressure up to 10^{-3} mbar, which is our experimental limitation. In this paper we present the results of the kinetics measurements. In a second paper we try to establish a connection between the kinetics and the adsorbate coverages on the Cu(110) surface [18].

2. Experimental

All experiments were conducted in a UHV system equipped with Auger electron spectroscopy (AES), low-energy electron diffraction (LEED), photoelectron emission microscopy (PEEM), and differentially pumped quadrupole mass spectrometry (QMS) for temperature-programmed desorption (TPD) and temperature-programmed reaction (TPR) spectroscopy. The system was operated as a continuous-flow reactor in the pressure range of 10^{-7} mbar to 10^{-3} mbar. The Cu(110) single crystal (1.5 mm thick, 9×11 mm^2) was held by two Ta wires which also served for resistive heating. The temperature was monitored by means of a chromel–alumel thermocouple. The Cu(110) surface was cleaned by repeated cycles of Ar^+ ion bombardment followed by annealing to 800 K until no traces of S, C, or O were detected by AES and a sharp (1×1) LEED pattern was observed. In situ AES showed that no impurities other than C- and O-containing adsorbates were present under the reaction conditions [18]. The reproducibility of the hysteresis measurements without additional cleaning cycles between measurements ruled out the buildup of a significant amount of coke deposits.

All gases were introduced via leak valves and a feedback-stabilized gas inlet system (MKS) that were also used to control the gases in pressure-ramping experiments. Calibration gases (H_2, H_2O, CO, formaldehyde, methanol, O_2, CO_2) were applied in order to relate the QMS signal to partial pressures. For water and methanol the vapor pressure over the liquid phase proved to be sufficient; for formaldehyde the vapor pressure of solid para-formaldehyde was taken. Oxygen of purity 5.0 and methanol of purity 2.8 were used.

From the detected masses ($m/e = 2$, 18, 28, 30, 31, 32, 44) the true partial pressures were calculated with a matrix inversion technique. From the pumping rates for the different gases, the flow rates also could be determined for each gas. Since the absolute partial pressures and the gas flows were obtained, the H-, O-, and C-mass balances could be checked for all TPR spectra presented here. Mass conservation for carbon checked by comparing the total consumption and total production was better than 5%; for oxygen and hydrogen the corresponding numbers were below 20%.

For kinetic measurements the sample was moved close to a cone, so that only gas molecules that were reflected from the sample could enter the cone and be detected by QMS. We can therefore determine the reactive sticking coefficient s_{reac} in situ from the measured partial-pressure variation of methanol and oxygen. Denoting the signal of a gas without reaction by I_0, we calculate the reactive sticking coefficient s_{reac} as

$$s_{\mathrm{reac}} = \frac{I_0 - I}{I_0}.$$

In our case we take the signal at 300 K for I_0, since a reaction rate of practically zero has been measured at this temperature.

3. Results and discussion

3.1. Temperature dependence

Fig. 1 shows a TPR spectrum obtained at a mixing ratio of $p(CH_3OH):p(O_2) = 1{:}0.6$ for $p(CH_3OH) = 1.0 \times 10^{-7}$ mbar. The TPR was recorded in a heating/cooling cycle in which a heating/cooling rate of 6 K/min was sufficiently slow to ensure that the reaction was close to steady-state conditions.

The reaction ignites at $\approx$400 K as the sample is heated. After passing a first peak, the reactivity drops and approaches a second high temperature peak at $T \geqslant 900$ K. Measurements with polycrystalline copper have shown that a maximum in reactivity is found at $\approx$900 K, which is slightly outside our accessible temperature range [16]. During cooling the reactivity extends down to $\approx$320 K. A pronounced hysteresis is thus present in the low-temperature range of the reaction below 500 K. The hysteresis is reproduced in a second cycle, which means that it cannot be caused by irreversible changes in the catalyst but rather has to be caused by differences in the adsorbate coverages and surface structure.

The top panel shows the reactive sticking coefficient, s_{reac}, of methanol as measured from the variation of the partial pressure of methanol. The reactive sticking coefficient is quite high, reaching 0.2 in the maxima of the catalytic activity. A similarly high sticking coefficient has been found by Bowker et al. in unstationary measurements [7,15]. The other panels demonstrate that all of the products expected from Eqs. (1)–(3) are seen in the experiment. The dominant product is formaldehyde, whose production accounts for $\geqslant$95% of the reacting methanol. Because of the high selectivity of the reaction for formaldehyde, the reactive sticking coefficient of methanol and the formaldehyde partial pressure are very similar in shape.

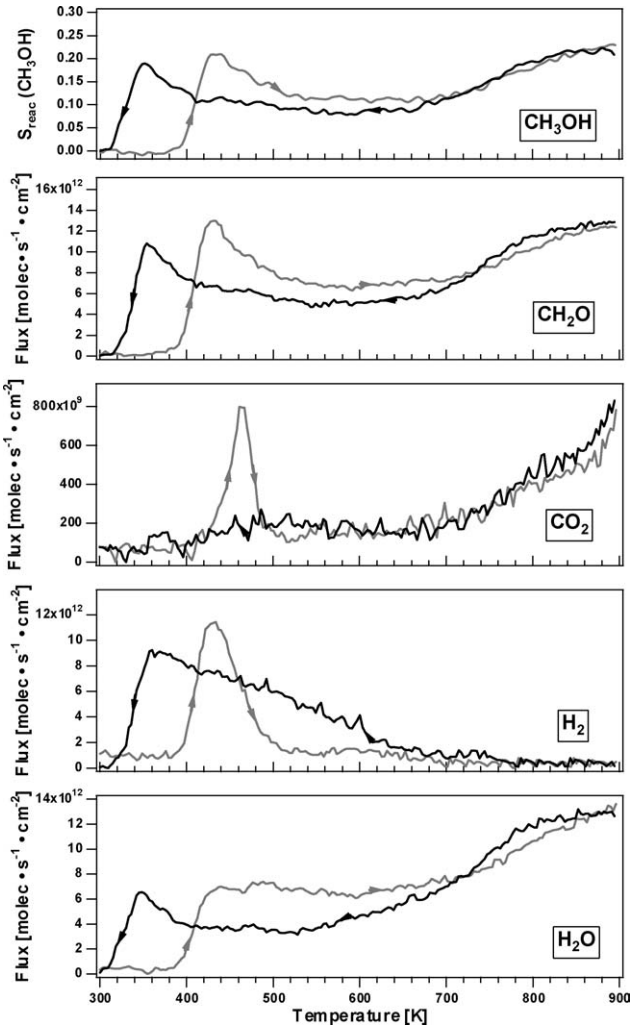

Fig. 1. Temperature programmed reaction spectroscopy in the 10^{-7} mbar range with $p(CH_3OH) = 1.0 \times 10^{-7}$ mbar, $p(CH_3OH):p(O_2) = 1{:}0.6$. Temperature up- and down ramping are indicated in each panel. The upper panel represents the reactive sticking coefficient of methanol, $s_{reac}(CH_3OH)$; the other panels indicate the production rates of the different products during methanol oxidation.

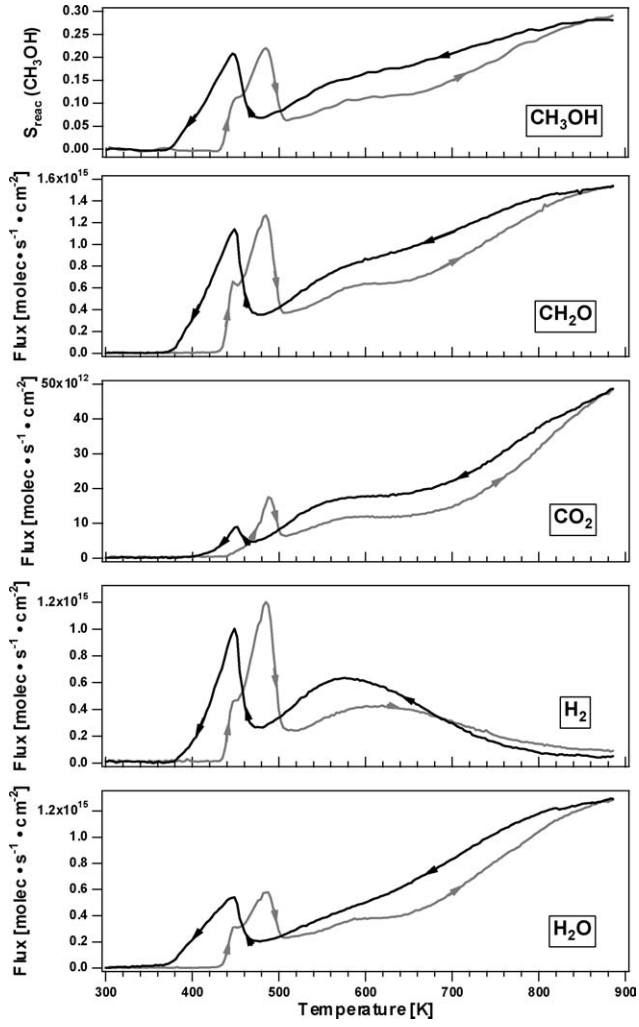

Fig. 2. Temperature programmed reaction spectroscopy in the 10^{-5} mbar range with $p(CH_3OH) = 1.0 \times 10^{-5}$ mbar, $p(CH_3OH):p(O_2) = 1{:}0.8$. Temperature up- and down ramping are indicated in each panel. The upper panel represents the reactive sticking coefficient of methanol, $s_{reac}(CH_3OH)$; the other panels indicate the production rates of the different products during methanol oxidation.

It can be seen that the CO_2 peak is present only during heating but not during the cooling part of the temperature cycle. Although the heating rate of 6 K/min is quite low, at 10^{-7} mbar transients may still contribute to the measured signal. This is the case for the CO_2 peak measured during heating between 400 and 500 K. A comparison with a TPD of a mixed $(5 \times 2) + (2 \times 1)$ layer (not shown here) [19] reveals that the amount of CO_2 produced in the CH_3OH/O_2 atmosphere is equal to the CO_2 desorption signal from the mixed overlayer. The CO_2 peak can be attributed to the decomposition and desorption of adsorbed formate; its intensity corresponds to a total amount of about half a monolayer. Therefore, we conclude that during the temperature up-ramping experiment formate represents a slowly accumulating adsorbate species that is not restored by the reaction once its decomposition and desorption of CO_2 set in. This interpretation is also supported by a separate experiment in which the heating ramp was stopped at 460 K and the CO_2 signal decayed to zero while the production rates for all other products remained steady.

The TPRS obtained in the 10^{-5} mbar range is displayed in Fig. 2. Note that the y-scale in each panel has been scaled to the increase in methanol pressure by two orders of magnitude compared with the experiment in Fig. 1. With the exception of the CO_2 peak, each of the low-temperature reaction peaks of the heating cycle consists of two components, as indicated by shoulders. In contrast to the 10^{-7} mbar range, at higher pressure all peak maxima of the products coincide. The CO_2 signal around 480 K consists of a shoulder followed by a single peak, which coincides with the higher of the double peaks of the other products. This indicates that the shoulder of the CO_2 peak coincides with the ignition of the first component of the double peak of the other reacting species, whereas the CO_2 production maximum and

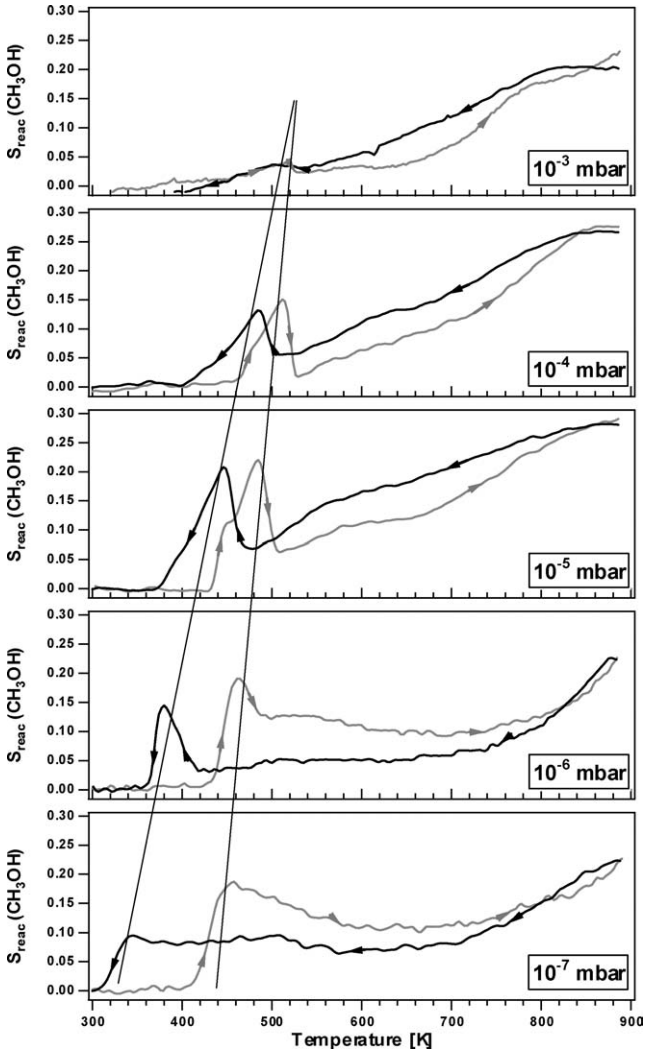

Fig. 3. Effect of the total pressure on the low temperature reactivity peaks in temperature cycling experiments. The methanol to oxygen gas mixture was always kept at $p(CH_3OH):p(O_2) = 1{:}0.8$ with only the total pressure being varied between 10^{-7} mbar and 10^{-3} mbar. The straight lines indicate systematic shifts in the peak positions with increasing total pressure.

the higher reaction peak proceed in concert. In contrast to the experiment in the 10^{-7} mbar range, the CO_2 peak in the 10^{-5} mbar range represents a stationary production rate and not a transient.

The other main effect of the pressure increase is that all of the low-temperature peaks between 300 and 500 K are shifted to higher temperatures and the separation of the different peaks during heating and cooling becomes smaller with increasing pressure. This is demonstrated in Fig. 3, where the total pressure has been varied systematically from 10^{-7} mbar to 10^{-3} mbar. The low-temperature reactivity peak shifts to a higher temperature by roughly 20 K per order of magnitude difference in pressure. With decreasing separation of the two reaction peaks, their amplitude becomes smaller until they completely vanish as they coalesce beyond 10^{-3} mbar. In agreement with the vanishing of the low-temperature reactivity peak at higher pressure, no such peak has been observed in studies at atmospheric pressure [20,21].

At the 10^{-5} mbar pressure range we can also see a clear structure in the H_2 production curve forming three distinct regions of the reaction: a narrow low-temperature peak, a broad maximum at intermediate temperatures between roughly 520 and 750 K, and a high-temperature region where no H_2 is produced.

Two competing reaction paths to formaldehyde formation via H_2 formation and without H_2 production can be formulated [7,15]:

$$4CH_3OH + O_2 \rightarrow 4CH_2O + 2H_2 + 2H_2O, \quad 520\ \text{K} < T < 750\ \text{K}; \tag{4}$$

$$2CH_3OH + O_2 \rightarrow 2CH_2O + 2H_2O, \quad T > 750\ \text{K}. \tag{5}$$

The different temperature ranges for each reaction path can be visualized with a plot of the ratio of CH_3OH to O_2 consumption versus the temperature. These results are displayed in Fig. 4 for different total pressures. The stoichiometry of the reaction relates the ratio of CH_2O to H_2O and H_2 to H_2O production, which are also shown. For comparison, the reactive sticking coefficient of methanol, representing the sum of the two pathways, is included in the same figure. We note that the peak positions in the TPRS vary strongly with the total pressure.

In the 10^{-5} mbar range the CH_3OH/O_2 consumption ratio is initially ≈ 2, then rises to ≈ 4, where it stays with some variation over 150–200 K before it drops again to ≈ 2. The ratio thus reflects three regimes of H_2 production. The three different regimes are indicated by hatched areas in the plot. In the 10^{-7} mbar range the distinction between the different regimes is less pronounced but still exists. In this pressure range we also observe strong hysteresis effects, as indicated by Fig. 4.

Under stationary conditions, in agreement with Eq. (4), the CH_3OH/O_2 consumption ratio of ≈ 4 corresponds to a substantial hydrogen production in the intermediate temperature range from ≈ 520 to ≈ 750 K. In the low-temperature range from 400 to 500 K, the ratio $r(H_2)/r(H_2O)$ reaches 2. From Eq. (4) it is clear that this ratio should not exceed 1. This discrepancy, which amounts to a factor of 2, reflects the well-known fact that a reliable calibration of the H_2 and H_2O signals is rather difficult. Reaction of water at the walls of the QMS chamber and dissociation of water at the QMS filament might be the reason for detecting a too high amount of H_2 with respect to the H_2O signal. It should be stressed that since all other gases are well calibrated, the overall mass balance, even for H and for O, remains within $\sim 20\%$ error.

The observation of hydrogen production in an intermediate-temperature regime, where chemisorbed oxygen was also present on the surface, was attributed by Bowker [7] to two possible causes: (i) a high activation barrier for water formation is present (referred to as an “energetic” reason in Ref. [7] or (ii) the reactants are organized in spatially separated regimes (referred to as a “structural” reason in Ref. [7]). In our experiments we see a pronounced hysteresis

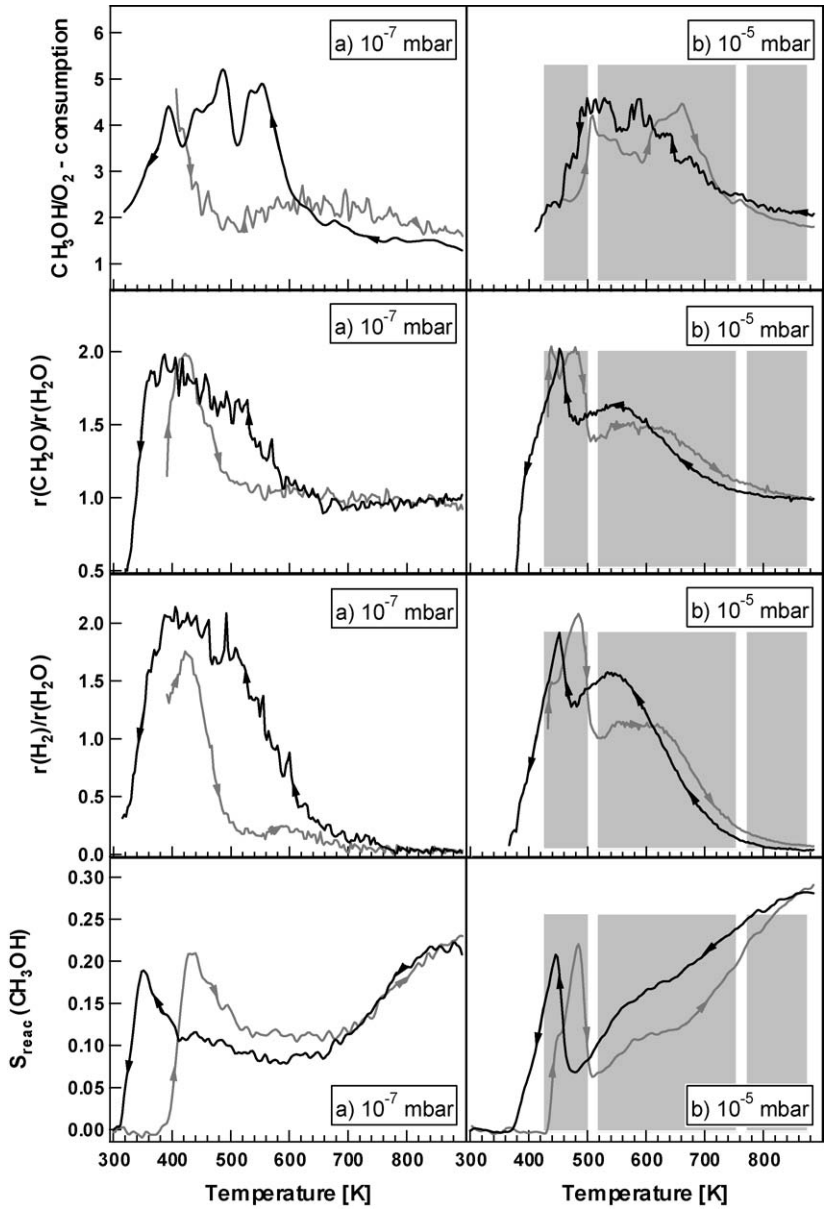

Fig. 4. Temperature dependence of the CH_3OH:O_2 consumption ratio and of the corresponding CH_2O:H_2O and H_2:H_2O production ratio in the 10^{-7} mbar and in the 10^{-5} mbar range. Different regimes of the reaction stoichiometry are represented as grey areas in (b). The reactive sticking coefficient of methanol is displayed in the lower panels in order to relate the different regimes to the reactivity of the surface.

that was several hundred Kelvin wide in product formation, including H_2 formation. This fact definitely rules out the explanation that the activation barrier is higher for water formation than for H_2 desorption. Evidently the second explanation (structural) holds, and island-forming processes leading to a separation of the reaction partners are responsible for the absence of water formation. This conclusion is corroborated by LEED/Auger data presented in the second part of this paper [18].

3.2. Dependence on the oxygen partial pressure

The dependence of the reaction rate on the oxygen partial pressure is shown in Fig. 5 for two temperatures, 480 and 850 K. In this experiment the methanol partial pressure was kept fixed at $p(CH_3OH) = 1 \times 10^{-5}$ mbar while the oxygen partial pressure was slowly cycled. The reaction is first order with respect to oxygen up to $\approx 6 \times 10^{-6}$ mbar, where the rate reaches a maximum. Beyond this point the rate decreases with increasing $p(O_2)$, and at high $p(O_2)$ the reactivity of the surface becomes quite small. Evidently high oxygen coverage inhibits the reaction. The position of the rate maximum varies only very little with the temperature, but the height increases from 480 to 850 K, and the inhibitory effect of oxygen is reduced in an intermediate $p(O_2)$ range between the rate maximum and $p(O_2) = 1 \times 10^{-5}$ mbar. The observed inhibitory effect of oxygen supports the reaction mechanism suggested by Bowker [7,15],

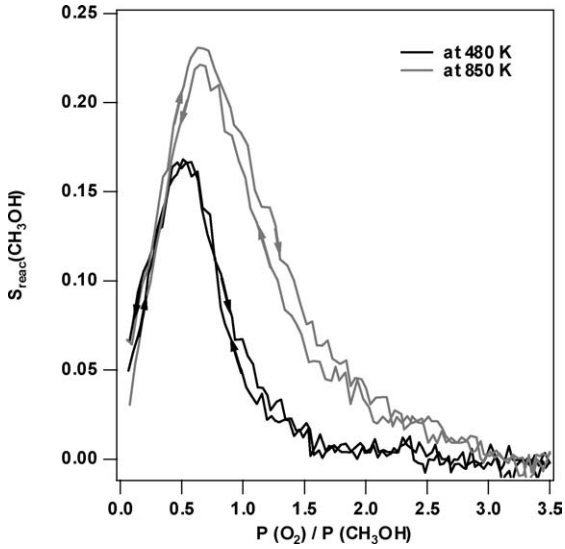

Fig. 5. Dependence of the reactive sticking coefficient of methanol, $s_{reac}(CH_3OH)$ on the oxygen partial pressure for $p(CH_3OH) = 1.0 \times 10^{-5}$ mbar. Shown are the data for two different temperatures, 480 and 850 K.

that only the edge oxygen adatoms of O-$p(2 \times 1)$ islands are active sites for methoxy formation, whereas the oxygen adatoms in the chains of O-$p(2 \times 1)$ islands are inactive.

The mixing ratio has a strong influence on the reaction kinetics as demonstrated by Fig. 6, which shows heating/cooling cycles with different methanol/oxygen ratios, $p(CH_3OH)/p(O_2)$. The optimum ratio for the low-temperature conversion as judged from the height of the peak around 420 K is a 1:0.6 ratio in the 10^{-7} mbar range, which shifts to a 1:0.8 ratio at 480 K with 10^{-5} mbar total pressure. With increasing oxygen content, ignition of the reaction shifts to higher temperature, but the conversion becomes low for too high oxygen partial pressures. This latter effect, which is particularly strong at high temperatures, is apparently caused by the inhibitory effect of high oxygen coverages.

4. Conclusion

The steady-state kinetics of methanol oxidation over Cu(110) has been studied at low pressure. Already at low pressure we find a high selectivity for the partial oxidation product formaldehyde. The reactivity of the surface at low and intermediate oxygen coverage is quite high, as indicated by a reactive sticking coefficient for methanol, which reaches 0.2. High oxygen coverage inhibits the reaction. The reactivity of the surface exhibits two peaks at low pressure: one around 400–520 K, which disappears when the total pressure exceeds 10^{-3} mbar, and a high-temperature peak around 900 K that persists at high pressure. Hydrogen production is observed in an intermediate temperature range, reflecting the presence of a second pathway with less oxygen consumption toward formaldehyde production.

Acknowledgment

This work was supported by the DFG under the priority program 1091 “Bridging the gap between ideal and real systems in heterogeneous catalysis.”

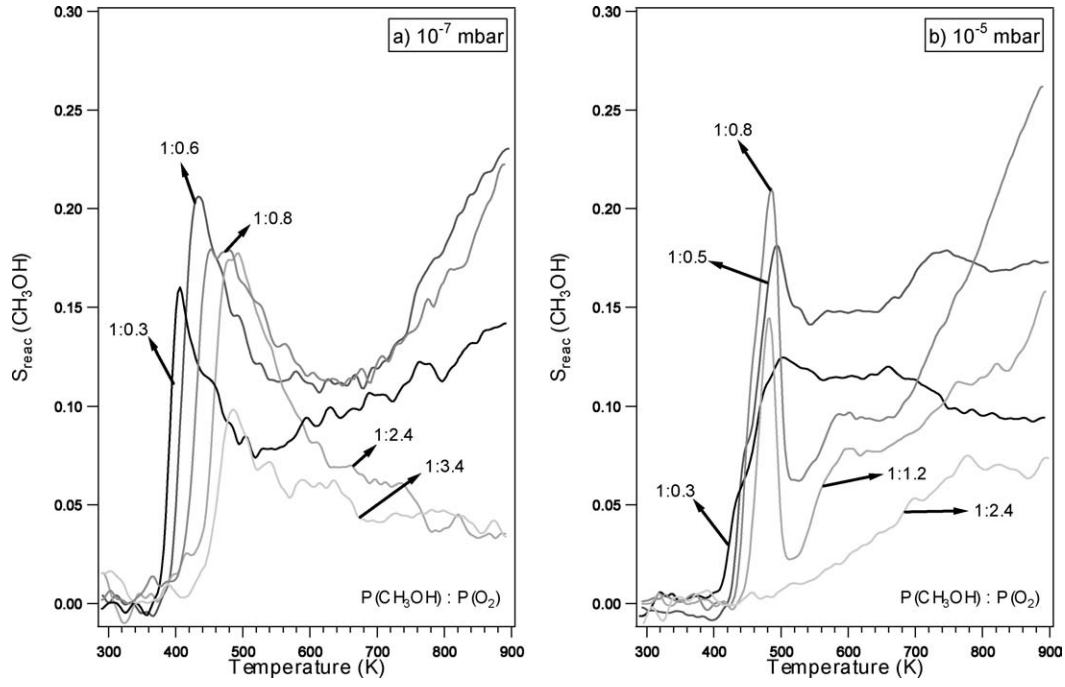

Fig. 6. Effect of the gas mixing ratio on methanol conversion over the Cu(110) surface in the 10^{-7} mbar (a) and the 10^{-5} mbar pressure range (b). The methanol conversion is given by the reactive sticking coefficient of methanol.

References

[1] J. Walker, Formaldehyde, Reinhold, Amsterdam, 1964;
J. Walker, Ullmann, Encyclopedia of Industrial Chemistry, Chemie, Weinheim, 1982.
[2] E. Jones, G. Fowlie, J. Appl. Chem. 3 (1953) 206.
[3] P.L. Hansen, J.B. Wagner, S. Helveg, J.R. Rostrup-Nielsen, B.S. Clausen, H. Topsoe, Science 295 (2002) 2053.
[4] M.M. Günter, T. Ressler, B. Bems, C. Büscher, T. Genger, O. Hinrichsen, M. Muhler, R. Schlögl, Catal. Lett. 71 (2001) 37.
[5] I.E. Wachs, R.J. Madix, J. Catal. 53 (1978) 208.
[6] A.F. Carley, A.W. Owens, M.K. Rajumon, M.W. Roberts, Catal. Lett. 37 (1996) 79.
[7] F.M. Leibsle, S.M. Francis, S. Haq, N. Xiang, M. Bowker, Surf. Sci. 315 (1994) 284.
[8] F.M. Leibsle, S.M. Francis, S. Haq, M. Bowker, Surf. Sci. 318 (1994) 46.
[9] S.L. Silva, R.M. Lemor, F.M. Leibsle, Surf. Sci. 421 (1999) 135.
[10] S.L. Silva, R.M. Lemor, F.M. Leibsle, Surf. Sci. 421 (1999) 146.
[11] A.F. Carley, P.R. Davies, G.G. Mariotti, S. Read, Surf. Sci. 364 (1996) 525.
[12] T. Schedel-Niedrig, T. Neisius, I. Böttger, E. Kitzelmann, G. Weinberg, D. Demuth, R. Schlögl, Phys. Chem. Chem. Phys. 2 (2000) 2407.
[13] A. Knop-Gericke, M. Hävecker, T. Schedel-Niedrig, R. Schlögl, Catal. Lett. 66 (2000) 215.
[14] A. Knop-Gericke, M. Hävecker, T. Schedel-Niedrig, R. Schlögl, Top. Catal. 10 (2000) 187.
[15] M. Bowker, Top. Catal. 3 (1996) 461.
[16] H. Werner, D. Herein, G. Schulz, U. Wild, R. Schlögl, Catal. Lett. 49 (1997) 109.
[17] I. Böttger, T. Schedel-Niedrig, O. Timpe, R. Gottschall, M. Hävecker, T. Ressler, R. Schlögl, Chem. Eur. J. 6 (2000) 1870.
[18] L. Zhou, S. Günther, R. Imbihl, J. Catal., submitted for press.
[19] P.R. Davies, G.G. Mariotti, J. Phys. Chem. 100 (1996) 19975.
[20] V.I. Bukhtiyarov, I.P. Prosvirin, E.P. Tikhomirov, V.V. Kaichev, A.M. Sorokin, V.V. Evstigneev, React. Kinet. Catal. Lett. 79 (2003) 181.
[21] I.P. Prosvirin, E.P. Tikhomirov, A.M. Sorokin, V.V. Kaichev, V.I. Bukhtiyarov, Kinet. Catal. 44 (2003) 662.